DALTON
FULL PAPER

Bis(acetylamido)oxovanadium(IV) complexes: solid state and solution studies

Debbie C. Crans,*[a] A. Raza Khan,[a] Mohammed Mahroof-Tahir,[ac] Sujit Mondal,[a] Susie M. Miller,[a] Agnete la Cour,[a] Oren P. Anderson,[a] Tamás Jakusch[b] and Tamás Kiss*[b]

[a] *Department of Chemistry, Colorado State University, Fort Collins, Colorado 80523-1872, USA*
[b] *Department of Inorganic and Analytical Chemistry, Jozsef Attila University, P.O. Box 440, Szeged, H-6701, Hungary*
[c] *Department of Chemistry, G.I.K. Institute of Eng. Sci. & Technology, Topi, N.W.F.P., Pakistan*

Received 22nd February 2001, Accepted 22nd February 2001
First published as an Advance Article on the web 31st October 2001

The syntheses, solid state, spectroscopic and potentiometric solution characterizations of $VO(acac\text{-}NH_2)_2$ (acac-NH_2 = acetylacetamido) and $VO(acac\text{-}NMe_2)_2$ (acac-NMe_2 = *N*,*N*-dimethylacetylacetamido) have been investigated. In $VO(acac\text{-}NMe_2)_2$ the vanadium ion exhibits a distorted square pyramidal coordination environment. Crystals of $VO(acac\text{-}NMe_2)_2$ are monoclinic and structural studies were carried out. EPR and UV-visible spectroscopic and potentiometric methods were used to characterize the speciation, complex stability and structures in both aqueous and organic solutions. $VO(acac\text{-}NH_2)_2$ and $VO(acac\text{-}NMe_2)_2$ each form two species in solution: a 1 : 2 and a 1 : 1 metal : ligand complex. The complexes formed from $VO(acac\text{-}NH_2)_2$ are slightly more stable than those of $VO(acac\text{-}NMe_2)_2$; however, $VO(acac)_2$ forms more stable complexes. In non-coordinating solvents the 1 : 2 complexes maintain a five-coordinate vanadium atom, whereas in coordinating solvents such as water and pyridine the complexes become six-coordinate. Based on the similarity of the EPR parameters of $VO(acac\text{-}NH_2)_2$ with those of the $VO(acac)_2$ complex, it is likely these species contain the coordinating solvent added *trans* to the V=O bond. These new $VO(acac)_2$ derivatives are improved with respect to water solubility. Although the solution stability is not as good as that of $VO(acac)_2$, it is higher than that of $VO(acac\text{-}R)_2$ (R = CH_3 or C_2H_5). Thus, should the stability of the 1 : 1 complex be important for the compound's efficacy, both of these new complexes would be predicted to be less effective than $VO(acac)_2$ but more effective than $VO(acac\text{-}Et)_2$ (acac-Et = 3-ethylacetylacetonate) in lowering glucose levels in streptozotocin-induced diabetic rats.

1.0 Introduction

A series of vanadium(IV) coordination complexes have been found to have promising therapeutic potential against type 2 diabetes.[1–8] The success of one of these compounds has led to clinical trials of KP-102, a compound related to $VO(malto)_2$ (malto = 3-hydroxy-2-methyl-4-pyrone).[1,2] The compounds successful in animal studies contain organic ligands with oxygen-donor,[1,3,4] nitrogen-donor, sulfur-donor,[5] mixed oxygen–nitrogen donor[6,7] and nitrogen–sulfur donor functionalities.[8] The therapeutic application of these compounds has rekindled the interest in vanadium(IV) compound synthesis, coordination chemistry, and speciation chemistry in solution.[9] We have recently found that $VO(acac)_2$ (acac = acetylacetonate) is as good as or better than $VO(malto)_2$ in lowering plasma glucose levels in streptozotocin-induced diabetic rats.[4]

$VO(acac)_2$ is a very well known compound[10,11] and has been used extensively as a catalyst in organic synthesis.[12–14] A wide range of derivatives has been reported most of which are not soluble in water.[15] As a result, we have been interested in developing new water soluble $VO(acac)_2$-derived complexes. The amide functionality has previously been characterized as coordinating in vanadium complexes,[16,17] suggesting that incorporation of such functionality in an $acac^-$ unit likely would lead to new and potentially interesting vanadium(IV) complexes. However, the Hacac-NR_2 (R = H or CH_3) ligand, $CH_3C(O)CH_2C(O)NR_2$, is an asymmetric variant of the Hacac ligand and has the possibility of forming isomeric metal complexes. The current manuscript describes the syntheses, solid state and solution characterization by spectroscopy and potentiometry of two new compounds with the general formula $VO(acac\text{-}NR_2)_2$ (R = H or CH_3).

2.0 Experimental

2.1 Materials and methods

All reagent grade chemicals for synthesis were obtained from Aldrich chemical company and used without further purification. The vanadyl sulfate preparations used were in general the trihydrate as determined by UV-vis spectroscopy. Chemicals used in pH-potentiometric measurements were Sigma or Aldrich products and the highest analytical purity available. In addition, the purity of the ligands was checked by NMR and the exact concentration of the ligand solutions was calculated by the Gran method.[18] Infrared (IR) spectra were recorded on a Perkin-Elmer 1600 FT-IR spectrometer in KBr pellets and/or in Nujol. Elemental (C, H and N) analyses were performed by Desert Analytics Laboratory at Tucson, Arizona.

2.2 Syntheses

$[VO(acac\text{-}NH_2)_2]$. *Method A.* Vanadyl sulfate trihydrate (1.0 g, 4.6 mmol) was dissolved in distilled water (15 mL) followed by the addition of acetoacetamide (1.40 g, 13.9 mmol) under constant stirring. A solution of 10% sodium bicarbonate was added dropwise to raise the pH of the solution from 1.8 to 3.6 where a suspension formed. A bluish precipitate formed on standing for a day at 4 °C. The precipitate was filtered off, washed with a small amount of chloroform and dried under

vacuum. Yield 0.92 g (76% based on $VOSO_4$) (Found: C, 35.60; H, 4.53; N, 10.21%. $C_8H_{12}N_2O_5V$ requires C, 35.96; H, 4.49; N, 10.49%). IR (Nujol, cm^{-1}): 3445 (NH), 3304 (CH), 3195 (CH), 1624 (C=O), 1575 (C=O), 1504 (C=O), 1314, 1195, 1079, 1032, 986, 973, 940, 804, 796, 766, 715, 683, 631.

Method B. Vanadyl sulfate trihydrate (2.0 g, 9.2 mmol) was dissolved in distilled water (20 mL) and the temperature slowly raised and maintained at 75 °C. A saturated solution of sodium acetate (2.60 g, 31.7 mmol) was added dropwise under constant stirring. After the pH of the solution was stabilized at 4.8 (±0.1), acetoacetamide (2.07 g, 20.5 mmol) in distilled water (5 mL) was added dropwise and the reaction mixture stirred for 30 min at 75 °C. A blue-greenish precipitate formed during the reaction period. The solution was cooled to ambient temperature, the precipitate filtered off, thoroughly washed with cold distilled water and dried under vacuum over phosphorus pentaoxide. Yield: 1.87 g (76% based on $VOSO_4$) (Found: C, 35.79; H, 4.61; N, 10.31%). IR (Nujol, cm^{-1}): 3449 (NH), 3316 (CH), 3200 (CH), 1622 (C=O), 1576 (C=O), 1506 (C=O), 1314, 1194, 1080, 1031, 976, 938, 794, 766, 717, 682, 630. IR (KBr, cm^{-1}): 3454 (NH), 3326 (CH), 3209 (CH), 2999 (CH), 1622 (C=O), 1578 (C=O), 1509 (C=O), 1482, 1426, 1370, 1344, 1198, 1085, 1040, 981, 943, 797, 768, 714, 686, 632, 567, 492.

[VO(acac-NMe_2)$_2$]. Vanadyl sulfate trihydrate (2.0 g, 9.2 mmol) was dissolved in distilled water (20 mL) and the temperature raised and maintained at 75 °C. A saturated solution of sodium acetate (2.60 g, 31.7 mmol) was added under constant stirring. After the pH of the solution was stabilized at 4.8 (±0.1), *N*,*N*-dimethylacetoacetamide (2.7 g, 16.7 mmol) in distilled water (2 mL) was added dropwise and the reaction mixture stirred for 30 min at 75 °C. After cooling at ambient temperature, the reaction mixture was extracted with benzene. Evaporating the benzene solvent to dryness under reduced pressure isolated the light blue crystalline product. Yield: 2.32 g (78% based on $VOSO_4$) (Found: C, 44.77; H, 6.33; N, 8.62%. $C_{12}H_{20}N_2O_5V$ requires C, 44.58; H, 6.19; N, 8.67%). IR (KBr, cm^{-1}): 3448 (CH), 2937 (CH), 1594 (C=O), 1570 (C=O), 1542 (C=O), 1507 (C=O), 1498, 1426, 1401, 1373, 1357, 1347, 1261, 1216, 1192, 1042, 988, 960, 774, 689, 635, 609, 507, 478.

2.3 Solid state characterization

Crystallographic studies of VO(acac-NMe_2)$_2$. Rectangular blue crystals of VO(acac-NMe_2)$_2$ were obtained in two ways: (a) by slow diffusion of hexane into a saturated solution of methylene chloride at −10 °C for one week; and (b) from a saturated benzene solution at 4 °C. Since only the latter crystals led to results suitable for publication, only these data have been included in the following discussion. X-Ray diffraction data were recorded on a Bruker AXS SMART CCD diffractometer employing Mo-Kα radiation (graphite monochromator). The structure was solved by Patterson methods and refined (on F^2 using all data) by a full-matrix, weighted least-squares process. Using anisotropic displacement parameters all non-hydrogen atoms were refined. Hydrogen atoms were placed in idealized positions and refined by using a riding model. Standard Bruker control (SMART) and integration (SAINT) software was employed, and Bruker SHELXTL[19] software was used for structure solution, refinement, and graphics. Details of the crystallographic experiments and computations are listed in Table 1.

CCDC reference number 157280.

See http://www.rsc.org/suppdata/dt/b1/b101718g/ for crystallographic data in CIF or other electronic format.

2.4 Solution characterization

Preparation of solutions for potentiometric studies. Solutions of Hacac-NH_2 and Hacac-NMe_2 were made from the pure compounds in distilled water. The purity of the ligands was checked by potentiometry and NMR spectroscopy. The stock solution of VO^{2+} was prepared as described previously,[20] and standardized for metal concentration by permanganate titration and for hydrogen ion concentration by potentiometry. The ionic strength was adjusted to 0.200 M KCl, and the temperature maintained at 25.0 ± 0.1 °C.

Potentiometric studies. The stability constants of the proton and vanadium(IV) complexes of Hacac-NH_2 and Hacac-NMe_2 were determined by pH potentiometric titration of 25.0 mL samples. The concentration of VO(IV) varied in the range 0.8–4 mM and the molar ratio between metal ion and the ligand was 1 : 1, 1 : 2, 1 : 4, 1 : 8, 1 : 12, 1 : 40 or 1 : 80. (Accurate pH potentiometric titrations could be made even in the presence of such high excesses of ligands, since the ligand dissociation processes taking place at significantly higher pH values do not buffer the system. Thus, the observed pH changes can be ascribed to metal/ligand interactions.) Titrations were performed from pH 2.0 until precipitation or slow equilibration; these problems occurred in the pH range 4–6 depending on the ligand and metal ion : ligand ratio. Titrations were carried out with 0.2 M KOH solution under a purified argon atmosphere. In some cases the pH equilibrium could not be reached within 10 min due either to precipitation or slow complex formation; these titration points were omitted from the calculation. The experiments were performed in duplicates and in all cases the reproducibility of the titration curves was within 0.005 pH unit. The pH was measured with an Orion HOA pH-meter equipped with a Metrohm 6.0234.100 combined pH glass electrode calibrated for hydrogen ion concentration.[21] The pK_w calculated from the strong acid and strong base titration was 13.755 ± 0.005.

The concentration stability constants, $\beta_{pqr} = [M_pA_qH_r]/[M]^p[A]^q[H]^r$, were calculated with the aid of the computer program PSEQUAD.[22] The formation of the hydroxo complexes of VO(IV) was taken into account. The four known species $[VO(OH)]^+$, $[(VO)_2(OH)_2]^{2+}$, $[VO(OH)_3]^-$ and $[(VO)_2(OH)_5]^-$ were used in the calculations (log $\beta_{10\text{-}1} = -5.94$, log $\beta_{20\text{-}2} = -6.95$, log $\beta_{10\text{-}3} = -18.0$ and log $\beta_{20\text{-}3} = -22.0$).[23] The stability constants were corrected for the different ionic strength using the Davies equation.

Solution preparation for EPR, ^{51}V NMR and UV-visible spectroscopic studies. EPR and UV-visible spectroscopy were employed to analyze sample solutions prepared from crystalline compounds. Concentrations ranging from 1.2 to 10 mM were used in DMF, DMSO, CH_3CN and pyridine and from 2.5 to 4.0 mM in aqueous solution. EPR and UV-visible studies were conducted in aqueous solutions of complex in the presence of 0 to 500 mM excess of ligands; solutions with excess of ligand were prepared by adding solid complex to a ligand solution. Both VO(acac-NH_2)$_2$ and VO(acac-NMe_2)$_2$ complexes dissolve slowly so suspensions were vortexed up to 30 minutes (preferred over sonication because this prevented heating of samples). The indicated times (or pH) reflect the times (or pH) from complete dissolution of the solid compound (with and without ligand). The samples were referenced and quantitated against aqueous vanadyl sulfate solutions in 0.1 M H_2SO_4; these solutions had been calibrated by their absorbances at 767.6 nm (ε 18.0 M^{-1} cm^{-1}).[24]

EPR spectroscopy. *Data acquisition.* The EPR spectra were recorded on a Bruker EMX 200 spectrometer. The first derivative X-band EPR spectra were recorded at ambient temperature in 1 mm quartz capillary tubes that were placed in 5 mm quartz EPR tubes. The spectra were recorded between 9.750 and 9.900 GHz (X-band) and at 40 mW microwave power. This microwave power setting was chosen in order to be able to quantitate the observed signals as described previously.[25] The parameters of acquisition were: a modulation frequency of 100.00 kHz, a modulation amplitude of 5.00 G, a time constant

of 164 ms, a sweep width of 2000 G, and a sweep time of 84 s. Four scans with 2048 points were recorded with a center field of 3500.00 G. The spectrometer center field was calibrated using a powdered sample of 2,2-diphenyl-1-picrylhydrazyl (DPPH) which has a g_0 factor of 2.0037 ± 0.0037.[26]

Quantitation of the vanadium concentrations was carried out by recording spectra of a series of standard solutions of $VOSO_4$ (from 0.36 to 5.0 mM). The signal recorded for the vanadyl cation ($pK_a = 5.9$)[23] is in agreement with that reported previously and represents $VO(H_2O)_5^{2+}$ and/or $VO(H_2O)_4(OH)^+$,[24] depending on the pH of aqueous sample solutions; these two species are collectively referred to as hydrated VO^{2+} species. Since the linewidths of the species vary, quantitation must involve integration of signals. Accordingly, it was important to record spectra for background correction.

Analysis of the EPR spectra. The EPR spectra were background corrected, and then, baseline adjustments were carried out using linear functions provided in the Bruker WINEPR System software (version 2.11). When the spectrum contained more than one species the spectrum was simulated using Bruker WINEPR SimFonia software (version 1.25) given the best fit of species and parameters for the complexes. Some differences in parameters were observed for VO^{2+} depending on whether the parameters were calculated directly from the spectra or from a simulated spectrum (presumably this reflects some differences in the second order correction terms which are applied differently by the two methods). When quantitating spins, both normalized double integration and peak-to-peak integration were used for determining the aqueous $VO(NR_2\text{-acac})_2$ concentration by comparison to a standard curve obtained with a series of reference $VOSO_4$ solutions (0.1 M H_2SO_4; ranging from 0.36 to 5.02 mM). The sample concentrations were measured in duplicate samples. The results reported in this manuscript are conservative average values and most were obtained using the double integration method, since this method is more reliable when solutions containing species with different linewidths are investigated. The errors on the formation constants were calculated using least squares analysis and the errors are indicated as ± SD.

^{51}V NMR spectroscopy. The ^{51}V NMR spectra were recorded on a Varian Inova-300 spectrometer at 78.9 MHz (7.0 T). The parameters used for the quantitative spectra were: a sweep width of 83600 Hz, a pulse width of 40° and an acquisition time of 0.096 s. The quantitative measurements were carried out in a 5 mm precision NMR tube with a 4 mm NMR insert capillary tube. A 3.4 mM ammonium metavanadate standard aqueous solution (pH 11.3) was poured into the precision insert capillary tube and placed in a precision 5 mm NMR tube which had a 5.0 mM ammonium metavanadate standard aqueous solution at pH 8.5. The concentration of vanadium(v) in the capillary tube was determined after recording the ^{51}V NMR spectrum and comparing the spectral integration of the signals with that from the reference solution. The aqueous solutions of $VO(acac\text{-}NH_2)_2$ prepared as described above were placed in the NMR tube outside the capillary and V(v) concentrations were calculated (compared to the concentration of a standard solution of ammonium metavanadate in the capillary tube) with an estimated 10% accuracy using the spectral integrations. Typically, 20,000 to 40,000 transients were required to obtain spectra with reasonable signal-to-noise.

UV-Visible spectroscopy. UV-Visible spectra were recorded on a Perkin-Elmer Lambda 4B spectrometer from 190 to 900 nm using a constant temperature bath (Haake A81) at 21 ± 1 °C. Solutions examined contained from 1.0 to 10 mM of crystalline $VO(acac\text{-}NH_2)_2$ and $VO(acac\text{-}NMe_2)_2$ dissolved in DMF, DMSO, pyridine and CH_3CN; $VO(acac\text{-}NH_2)_2$ is insoluble in this solvent. In aqueous solution (from 2.5 to 4.18 mM) crystalline $VO(acac\text{-}NH_2)_2$ and $VO(acac\text{-}NMe_2)_2$ were dissolved in distilled water and in distilled water containing ligand. Unless otherwise indicated, spectra were recorded immediately after complete dissolution.

3.0 Results and discussion

3.1 Synthesis of complexes

Two amide analogs of Hacac were used to prepare derivatives of $VO(acac)_2$, *i.e.* $VO(acac\text{-}NH_2)_2$ and $VO(acac\text{-}NMe_2)_2$, from amide ligand and vanadyl sulfate (trihydrate). The well known synthesis of $VO(acac)_2$ from $VOSO_4$ and Hacac was initially used to prepare the parent complex with pH maintained around 4.0 by using an aqueous solution of sodium bicarbonate.[27] The product precipitated out of the cooled solution in optimum yield of 76%. Although this method can generate product in high yields, the yield is very sensitive to the pH (undesired insoluble vanadyl hydroxides form when the pH is increased above 5–6). The need for careful pH control led us to pursue alternative and improved procedures for preparation of these compounds. A method that enforces strict pH control by use of a buffer would avoid decomposition of the product and/or the formation of vanadyl hydroxides. Accordingly, a synthetic procedure was developed by using a CH_3CO_2H/CH_3CO_2Na buffer system. The choice of acetate buffer is particularly appropriate since CH_3CO_2H has a pK_a value of ≈4.8 and vanadyl acetate is a known compound.[28] The blue vanadyl sulfate solution turned dark gray upon addition of sodium acetate indicative of the acetate complex formation. The $VO(acac\text{-}NH_2)_2$ complex repeatedly precipitated in high (76%) yield from acetate-buffered solution after the addition of the ligand and stirring in air for 30 min at 75 °C. The color of the semicrystalline plate like solid was greenish blue; however, when the crystal was ground to a powder, the color was blue. This procedure was also used for the preparation of the $VO(acac\text{-}NMe_2)_2$ complex; the higher water solubility of this complex favored isolation of the product by extraction with benzene. Upon evaporation of the benzene under reduced pressure, blue crystalline and analytically pure $VO(acac\text{-}NMe_2)_2$ was isolated in high (78%) yield.

3.2 Infrared spectroscopy

The solid-state properties of $VO(acac\text{-}NH_2)_2$ and $VO(acac\text{-}NMe_2)_2$ were examined by infrared spectroscopy and details are given in the Experimental section. Two signals were observed in the region of ν(V=O) stretches for $VO(acac\text{-}NH_2)_2$ (943 and 981 cm^{-1}) and for $VO(acac\text{-}NMe_2)_2$ (960 and 988 cm^{-1}) were observed, which are close to ν(V=O) stretches reported for other related oxovanadium(IV) derivatives.[25,29]

3.3 Crystallographic characterization of $VO(acac\text{-}NMe_2)_2$

Data for two crystals, one prepared from slow diffusion of hexane into a saturated solution of the complex in CH_2Cl_2 (−10 °C) and the other from a saturated solution of benzene (4 °C), were obtained. Significant disorder in the structure of the former prevented satisfactory refinement; the second structure contained a disordered benzene molecule not readily amenable to modeling. Fig. 1 shows the structure and the atom labeling scheme for $VO(acac\text{-}NMe_2)_2$ for the crystal obtained from benzene. Selected interatomic distances and angles are shown in Table 2.

$VO(acac\text{-}NMe_2)_2$ exists as a discrete mononuclear complex with the vanadium atom in a distorted square pyramidal coordination environment. Two oxygen atoms of each of the $NMe_2\text{-}acac^-$ ligands coordinate to the vanadium in the equatorial plane. The oxo group occupies the apical position and the vanadium atom lies 0.59 Å above the least-squares equatorial plane through O2, O3, O4, and O5. This distortion is similar to those reported for $VO(acac)_2$ (0.55 Å),[11] $VO(acac\text{-}Et)_2$

Table 1 Details of the crystallographic experiments and computations for $VO(acac\text{-}NMe_2)_2$

Molecular formula	$C_{18}H_{26}N_2O_5V$
M	401.35
Crystal system	Monoclinic
Space group	$P2_1/n$
a/Å	7.005(2)
b/Å	19.610(6)
c/Å	14.601(4)
β/°	90.19(2)
V/Å^3	2005.5(10)
Z	4
Radiation (λ/Å)	Mo-Kα (0.71073)
μ/mm^{-1}	0.524
Reflections collected	10311
Independent reflections	4767
R ($[I > 2\sigma(I)]$)	0.061
R_w (all data)	0.182

Table 2 Selected interatomic distances (Å) and angles (°) for $VO(acac\text{-}NMe_2)_2$

V–O(1)	1.597(2)	V–O(3)	1.958(2)
V–O(4)	1.958(2)	V–O(5)	1.966(2)
V–O(2)	1.976(2)	C(1)–O(2)	1.278(4)
C(1)–C(2)	1.427(4)	C(2)–C(3)	1.379(4)
N(2)–C(7)	1.351(4)	O(3)–C(3)	1.296(4)
C(3)–C(4)	1.507(5)	O(4)–C(9)	1.297(4)
O(5)–C(7)	1.284(4)	C(7)–C(8)	1.440(4)
C(8)–C(9)	1.373(5)	C(9)–C(10)	1.511(4)
O(1)–V–O(3)	107.52(11)	O(1)–V–O(4)	107.54(11)
O(3)–V–O(4)	84.35(10)	O(1)–V–O(5)	107.36(11)
O(3)–V–O(5)	145.08(10)	O(4)–V–O(5)	86.75(9)
O(1)–V–O(2)	107.48(11)	O(3)–V–O(2)	86.57(9)
O(4)–V–O(2)	144.96(10)	O(5)–V–O(2)	81.63(9)
O(2)–C(1)–N(1)	116.6(3)	O(2)–C(1)–C(2)	122.5(3)
N(1)–C(1)–C(2)	120.9(3)	C(3)–C(2)–C(1)	121.9(3)
C(1)–O(2)–V	130.8(2)	C(3)–O(3)–V	128.2(2)
O(3)–C(3)–C(2)	126.1(3)	O(3)–C(3)–C(4)	113.9(3)
C(2)–C(3)–C(4)	120.0(3)	C(9)–O(4)–V	128.3(2)
C(7)–O(5)–V	130.6(2)	O(5)–C(7)–N(2)	116.5(3)
O(5)–C(7)–C(8)	122.8(3)	N(2)–C(7)–C(8)	120.7(3)
C(9)–C(8)–C(7)	121.4(3)	O(4)–C(9)–C(8)	126.2(3)
O(4)–C(9)–C(10)	114.1(3)	C(8)–C(9)–C(10)	119.6(3)

Symmetry transformation used to generate equivalent atoms: $0.5 - x$, $0.5 + y$, $0.5 - z$.

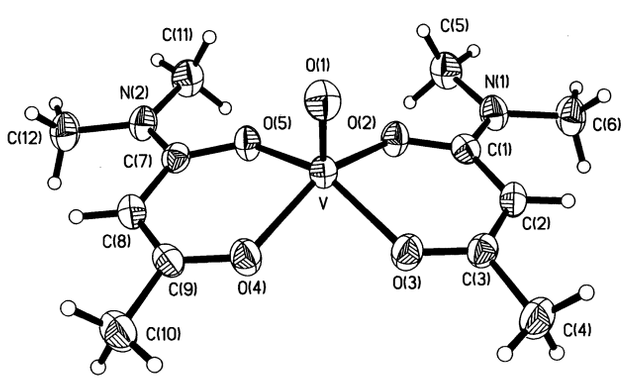

Fig. 1 X-Ray crystallographic structure and atomic labeling of $VO(acac\text{-}NMe_2)_2$.

(acac-Et = 3-ethylacetylacetonate) (0.56 Å),[25] $VO(acac\text{-}Me)_2$ (acac-Me = 3-methylacetylacetonate) (0.55 Å),[25] VO(acen) (acen = *N*,*N*′-ethylenebis(acetylacetoneiminate)) (0.58 Å),[29] and $VO(bzac)_2$ (bzac = 1-phenyl-1,3-butanedionate) (0.54 Å).[15]

The V–O(1) bond length of 1.597(2) Å is similar to the reported values for related complexes, including $VO(bzac)_2$ (1.612(10) Å),[15] $VO(acac\text{-}Et)_2$ (1.605(2) Å),[25] and $VO(acac\text{-}Me)_2$ (1.592(2) Å).[25] This bond distance is longer than the V=O bond in $VO(acac)_2$ (1.561(10) Å),[11] reflecting the increase in

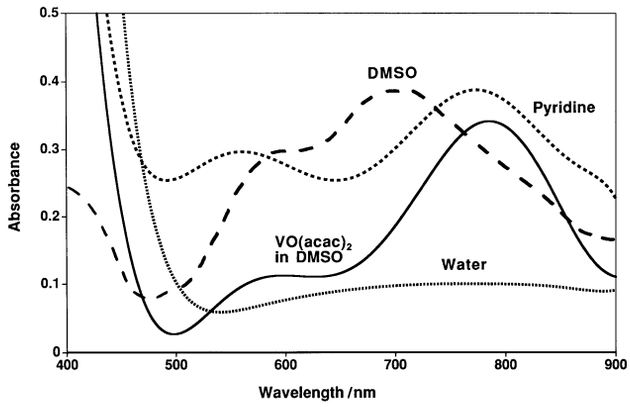

Fig. 2 UV-visible spectra of $VO(acac\text{-}NH_2)_2$ in (9.22 mM) DMSO, (3.55 mM) water and (8.73 mM) pyridine. The UV-visible spectrum of 8.36 mM $VO(acac)_2$ in DMSO is shown for comparison.

electron-donating abilities of the $acac\text{-}NMe_2^-$ ligand. The bond distances of V–O(2) 1.976(2), V–O(3)/V–O(4) 1.958(2) and V–O(5) 1.966(2) Å are significantly longer than the V=O bond length, as expected. Comparison of V–O bond lengths with the corresponding values in $VO(acac)_2$, $VO(acac\text{-}Me)_2$ and $VO(acac\text{-}Et)_2$ show that they are in the same range. The asymmetry in the amide ligand is reflected by a significant difference from the sets of V–O bond lengths in the $VO(acac)_2$[11] and the $VO(acac\text{-}Me)_2$[25] complexes; in contrast these bond lengths are very similar to those in the $VO(acac\text{-}Et)_2$ complex. Different bond lengths are observed for the C–C bonds in the conjugated framework in the amide (1.373(5) Å/1.379(4) and 1.427(4)/1.440(4) Å) than for $VO(acac)_2$, $VO(acac\text{-}Me)_2$ and $VO(acac\text{-}Et)_2$. Perhaps the most interesting aspect of this structure is the fact that the amide oxygen atoms are coordinated *cis* to the vanadium.

3.4 UV-Visible and EPR solution studies of $VO(acac\text{-}NH_2)_2$ and $VO(acac\text{-}NMe_2)_2$ in organic solvents

Solutions of crystalline $VO(acac\text{-}NH_2)_2$ and $VO(acac\text{-}NMe_2)_2$ generated ambient temperature EPR spectra with one species with experimentally indistinguishable parameters in DMF, in DMSO and in pyridine ($A_0 = (94\text{–}96) \times 10^{-4}$ cm^{-1}, $g_0 = 1.972\text{–}1.975$, Table 3). Similar parameters were observed for $VO(acac\text{-}NMe_2)_2$ in CH_3CN ($VO(acac\text{-}NH_2)_2$ was insoluble in CH_3CN). In all these solvents, only one species was observed even when examining solutions with low concentrations of complexes. These parameters are very similar to those observed for $VO(acac)_2$ in DMF, in pyridine, and in CH_3CN,[30] suggesting that the species forming are structurally and electronically similar to the major 1 : 2 $VO(acac)_2$ complex. Further to characterize these complexes, the UV-visible spectra were recorded (Fig. 2). Two peaks were observed in UV-visible spectrum for both $VO(acac\text{-}NH_2)_2$ and $VO(acac\text{-}NMe_2)_2$ at around 581 nm and at around 660–690 nm, although the absorption coefficients were slightly higher for $VO(acac\text{-}NH_2)_2$ in DMSO and pyridine. The spectral features are very similar to those reported for $VO(acac)_2$ in acetonitrile.[31]

However, distinct differences between the Hacac-amide and the Hacac systems were observed in DMF and DMSO. $VO(acac)_2$ in DMF and DMSO shows absorbance peaks at around 590 and 769 nm in these solvents (Fig. 2).[31] The shift of the high wavelength absorbance maximum from 700 to 769 nm for $VO(acac)_2$ has been attributed to solvent coordination to the vanadium atom.[31] With the vanadium–acac-NR_2 derived complexes, no shift of the absorbance maxima was observed, suggesting that no solvent coordination of DMF or DMSO takes place. However, in pyridine, $VO(acac)_2$,[31] $VO(acac\text{-}NH_2)_2$ and $VO(acac\text{-}NMe_2)_2$ yield absorbance maxima at around 580 and at around 770 nm (Fig. 2). This red shift of the absorbance

Table 3 The EPR and UV-visible parameters for speciation observed for $VO(acac\text{-}NR_2)_2$ and $VO(acac)_2$

Complex	$10^4 A_0/cm^{-1}$, g_0, λ_{max}/nm ($\varepsilon/M^{-1}\ cm^{-1}$)[a]				
	Water	Pyridine	DMSO	DMF	CH_3CN
$VO(acac\text{-}NH_2)_2$ (R = H)	92, 1.971 (1 : 2 species)[b] 550(36),[c] 826(54)[b] 101, 1.973 (1 : 1 species)[b] 800(83)[b]	95, 1.972 573(35) 773(44)	94, 1.973 583(28) 695(36)	96, 1.973 581(28) 662(33)	N/A (insoluble)
$VO(acac\text{-}NMe_2)_2$ (R = Me)	92, 1.972 (1 : 2 species)[b] 567(12),[c] 803(30)[b] 99, 1.972 (1 : 1 species)[b] 774(24)[b]	95, 1.973 585(22) 770(30)	94, 1.975 585(26) 690(33)	96, 1.973 558(34) 668(37)	96, 1.973 585(33) 687(41)
$VO(acac)_2$	92, 1.970[d] (*trans* 1 : 2 H_2O adduct) 570(20), 820(50)[d] 97, 1.970[d] (*cis* 1 : 2 H_2O adduct) 101, 1.970[d] (1 : 1 species) 645(20)[d]	96, 1.970[c] 578, 764[e]	588, 779[e]	96, 1.968[c] 590, 769[e]	97, 1.969[c] 593, 700[e]

[a] The experimental uncertainties are as follows: A_0 ($\pm 1 \times 10^{-4}$ cm^{-1}), g_0 (± 0.001), λ_{max} (± 3 nm) and ε (± 3 $M^{-1}\ cm^{-1}$). [b] The parameters have been obtained from solutions as described in detail in the text. [c] Ref. 30. [d] Ref. 25. [e] Ref. 31.

Table 4 Stability constants of the proton dissociation (pK_a) and VO(IV) complex formation ($\log \beta$) of Hacac-NH_2 and Hacac-NMe_2 at $T = 25$ °C and at $I = 0.2$ M (KCl)[a]

Equilibrium	Hacac-NH_2	Hacac-NMe_2	Hacac
$Hacac\text{-}NR_2 \rightleftharpoons (Hacac\text{-}NR_2)H_{-1} + H^+$	−10.62(1)	−13.3(1)	−8.76
$VO^{2+} + Hacac\text{-}NR_2 \rightleftharpoons VO(Hacac\text{-}NR_2)H_{-1} + H^+$	−2.30(4)	−2.34(3)	−0.03
$VO^{2+} + 2\ Hacac\text{-}NR_2 \rightleftharpoons VO((Hacac\text{-}NR_2)H_{-1})_2 + 2H^+$	−6.04(12)	−6.46(8)	−1.25
No. of points	200	212	—
Fitting[b]	6.53×10^{-3}	5.36×10^{-3}	—
$VOLH^{-1} + L \rightleftharpoons VOL_2H_{-2} + H^+$	−3.74	−4.12	−1.22
$\log K(VOLH_{-1}/VOL_2H_{-2})$	1.44	1.78	1.19
Ref.	This work	This work	32

[a] Errors indicate ±3 SD. [b] The average difference between the calculated and the experimental titration curves expressed in mL of titrant.[32]

maxima indicates that pyridine is a sufficiently strong ligand to coordinate to VO(IV) in all these complexes. Lack of coordination of the highly nucleophilic DMF and DMSO to the 1 : 2 $VO(acac\text{-}NR_2)_2$ species suggests that the vanadium atom is less electrophilic which further implies that the acac-NR_2^- ligands are significantly more electron donating than the $acac^-$ ligand. The amide N lone pair is delocalized to the amide oxygen which results in an overall decrease of the formation of the tautomeric enol. The possibility that steric hindrance of the NMe_2 group is preventing approach by the solvent is less likely since such steric hindrance is not present in the parent acac-amide system which also does not support DMF/DMSO coordination.

3.5 Potentiometric speciation in aqueous solution

The evaluation of the titration of the VO^{2+}–Hacac-NH_2 and VO^{2+}–Hacac-NMe_2 systems yielded the stability constants given in Table 4. The dissociation constant of Hacac-NH_2 ($pK_a = -10.62$) is higher than the appropriate constant of Hacac ($pK_a = -8.76$) and very similar to that of Hacac-Me ($pK_a = 10.60$).[32] Since the tautomeric enol is most acidic, these pK_a values show that the amide group is impeding the formation of the tautomeric enol, as found similarly for the alkyl group in the case of Hacac-Me and Hacac-Et.[32] The pK_a value of the Hacac-NMe_2 ($pK_a = -13.3$) is rather high and thus can only be determined with low accuracy. To avoid including too high an uncertainty in the formation constants of the vanadium(IV) complexes, the formation constants were tied to the characteristic proton displacement constants: $VO^{2+} + Hacac\text{-}NR_2 \rightleftharpoons VO(acac\text{-}NR_2)^+ + H^+$ and $VO^{2+} + 2\ Hacac\text{-}NR_2 \rightleftharpoons VO(acac\text{-}NR_2)_2 + 2H^+$. For the sake of comparison, the data were treated equally for both Hacac-NR_2 systems studied.

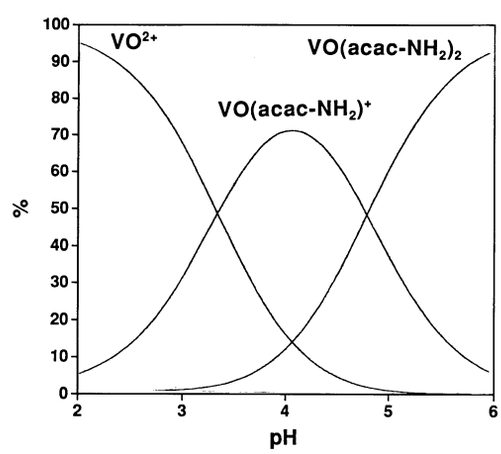

Fig. 3 Speciation diagram of the VO(IV)–Hacac-NH_2 system, $c(VO(IV)) = 0.001$ M (where $c(VO(IV))$ refers to the concentration of VO(IV) added to the solutions) with a VO^{2+}: Hacac-NH_2ratio of 1 : 80.

The metal–ligand systems could be described by the two complexes $VO(acac\text{-}NR_2)^+$ (also referred to as the 1 : 1 species) and $VO(acac\text{-}NR_2)_2$ (also referred to as the 1 : 2 species) where the dissociation constants refer to the reaction $VO(Hacac\text{-}NR_2) \rightleftharpoons VO(acac\text{-}NR_2) + H^+$. The speciation diagrams obtained for the VO^{2+}–Hacac-NH_2 and VO^{2+}–Hacac-NMe_2 systems (Figs. 3 and 4) are very similar. In both cases, up to a 1 : 10 fold excess of the ligands (less than 1 : 10), precipitation occurred before the formation of species $VO(acac\text{-}NR_2)_2$ was observed (data not shown). However, at 1 : 80 metal ion to ligand ratio, the amount of the 1 : 2 complex could reach 80% of total VO(IV). The $\log \beta$ values of $VO(Hacac\text{-}NH_2)H_{-1}$ are almost identical for Hacac-NH_2 and Hacac-NMe_2, but are

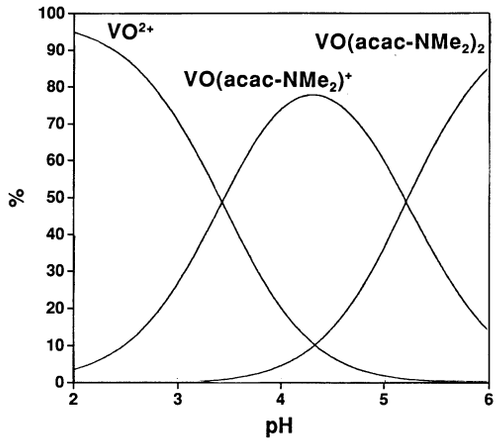

Fig. 4 Speciation diagram of the VO(IV)–Hacac-NMe_2 acac system, c(VO(IV)) as in Fig. 3, with a VO^{2+} : Hacac-NMe_2 ratio of 1 : 80.

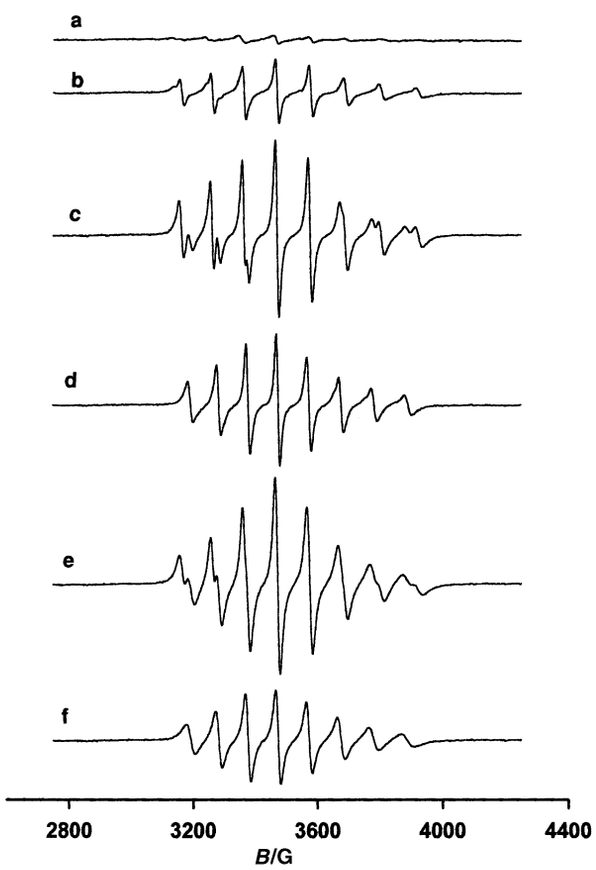

Fig. 5 EPR spectra of (a) 3.55 mM VO(acac-NH_2)$_2$ at pH 3.9, (b) 3.84 mM VO(acac-NH_2)$_2$ and 51.14 mM excess ligand at pH 3.9, (c) 2.91 mM VO(acac-NH_2)$_2$ and 427 mM excess ligand at pH 3.9, (d) 2.70 mM VO(acac-NH_2)$_2$ and 408 mM excess ligand at pH 8.1, (e) 3.86 mM VO(acac-NMe_2)$_2$ and 864 mM excess ligand at pH 5.3 and (f) 2.40 mM VO(acac-NMe_2)$_2$ and 1143 mM excess ligand at pH 9.2.

less than corresponding values for Hacac (see Table 4).[32] The difference in the constant of the two amide ligands characteristic of the equilibrium VO(acac-NR_2)$^+$ + Hacac-NR_2 $\rightleftharpoons$ VO(acac-NR_2)$_2$ + H^+ is much more obvious; the species VO(acac-NH_2)$_2$ is formed about 0.3 pH unit higher with the dimethyl derivative (Figs. 3 and 4). The spatial requirements of the methyl groups can impede binding of the second ligand to the metal ion; similarly in case of Hacac-NH_2 log K(VO(acac-NR_2)/VO(acac-NR_2)$_2$) is also higher than for the related systems. These observations confirm the expectation that the presence of the amide group in the ligand disfavors the formation of the enol ligand tautomer and also the two vanadium complexes.

3.6 Aqueous spectral studies of VO(acac-NH_2)$_2$

Further to explore the nature of the 1 : 2 and 1 : 1 complexes, spectroscopic studies were carried out. Dissolution of crystalline VO(acac-NH_2)$_2$ in distilled water (3.55 mM, pH 3.9) showed two species by EPR spectra (Fig. 5). The minor species (≈10%) has the parameters $A_0 = 101 \times 10^{-4}$ cm^{-1}, $g_0 = 1.973$ and the major species (≈90%) was identified as VO^{2+} ($A_0 = 106 \times 10^{-4}$ cm^{-1}, $g_0 = 1.964$)[24] and shows that VO(acac-NH_2)$_2$ hydrolyzes in aqueous solution. The former species corresponds to the 1 : 1 species described in the potentiometric studies. The addition of excess of ligand indeed decreased the concentration of VO^{2+} (Fig. 5). When 280 mM excess ligand was added a second species ($A_0 = 92 \times 10^{-4}$ cm^{-1}, $g_0 = 1.971$) was observed (data not shown) but no further change in speciation was observed even when 427 mM excess ligand was added (Fig. 5). In another sample preparation, at 408 mM excess ligand, the pH was increased to 8.1. Under these conditions the 1 : 2 species was the only observed species (Fig. 5).

Quantitative EPR studies were carried out to substantiate the potentiometric studies above. In solutions of crystalline VO(acac-NH_2)$_2$ approximately 20% of the vanadium(IV) was visible by EPR spectroscopy (Fig. 5). No change in the observed ratio of species by EPR was observed in these solutions after 24 h. In the solution containing 280 mM excess ligand a total of 97% of the vanadium(IV) added to the solution was observed. Dissolution of crystalline VO(acac-NH_2)$_2$ in solutions of free Hacac-NH_2 generated solutions with increasing vanadium(IV) species as evidenced by the decreasing signal to noise in the spectra with excess of free ligand (Fig. 5). In the spectrum containing 280 mM excess ligand 20% is present as the 1 : 2 complex and 80% as the 1 : 1 complex. The small fraction of the 1 : 2 species in the solution that forms from the crystalline compound shows that the complex is not as stable as VO(acac)$_2$ at this pH. The combination of quantitative EPR and ^{51}V NMR showed that a significant concentration of EPR-silent vanadium(IV), presumably in the form of soluble vanadium(IV)–hydroxo complexes, was present in these solutions in the absence of large amounts of ligand. (Some complex did oxidize and was observed as vanadium(V) oxoanions in solution (see below).) By quantitative EPR spectroscopy, a pH-dependent formation constant calculated as [1 : 1 complex]/[VO^{2+}][Hacac-NH_2] was measured to be 50 ± 10 M^{-1} at pH 3.9 and a formation constant calculated as [1 : 2 complex]/[1 : 1 complex][Hacac-NH_2] was measured to be 1.0 ± 0.2 M^{-1} at pH 3.9. These values are in fairly good agreement with the stability constants calculated for this pH from the potentiometrically determined stability constants: log K(1 : 1) = 40 and log K(1 : 2) = 1.5.

Evidence for these two complexes also was obtained by UV-visible spectroscopy. Solutions of crystalline VO(acac-NH_2)$_2$ in the presence of 99 mM excess ligand contained 1.9 mM 1 : 1 species and 0.22 mM 1 : 2 species. The spectrum in Fig. 6 represents the total absorption of 3.5 mM vanadium(IV). Since no ^{51}V NMR signal was observed for these solutions, the additional 1.4 mM was assigned to EPR-silent vanadyl hydroxides. Unfortunately, the EPR-silent vanadyl hydroxides are poorly characterized by UV-visible spectroscopy and prevent ruling out the possibility that some of the absorption in Fig. 6 is due to these species.[24] When crystalline VO(acac-NH_2)$_2$ is dissolved in solutions containing about 400 mM Hacac-NH_2 two absorbance maxima at 550 and 826 nm are added to the spectrum generated by the 1 : 1 species (Fig. 6). The red shift of the 826 nm absorbance maximum is consistent with coordination of a water molecule to the 1 : 2 complex as observed in VO(acac)$_2$ at 820 nm.[25] Using the EPR spectroscopic quantitation of the species in these solutions and assuming the observed absorptions are due to EPR-active complexes, absorption coefficients could be calculated (Table 3). These values represent maximum values since any absorption by the

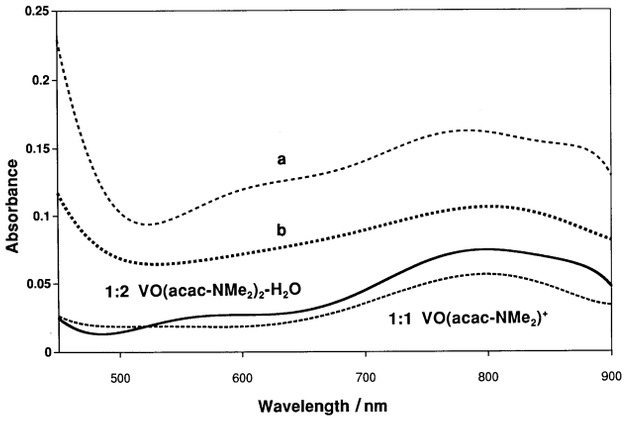

Fig. 6 UV-Visible spectra of (a) 3.6 mM VO(acac-NH_2)$_2$ and 99 mM excess ligand corresponding to 1.92 mM 1 : 1 species and 0.22 mM 1 : 2 species at pH 3.9, (b) 2.70 mM VO(acac-NH_2)$_2$ and 408 mM excess ligand corresponding to 1.9 mM 1 : 2 species at pH 8.1, (c) a simulated spectrum of 2.4 mM 1 : 1 species of VO(acac-NMe_2)$_2$ at pH 3.8 (calculated from a spectrum of 3.8 mM VO(acac-NMe_2)$_2$ and 436 mM excess ligand corresponding to 3.6 mM 1 : 1 species and 0.20 mM 1 : 2 species at pH 3.8) and (d) 2.4 mM VO(acac-NMe_2)$_2$ and 1143 mM excess ligand corresponding to 2.4 mM 1 : 2 species at pH 9.2.

EPR-silent species decreases the observation of the 1 : 1 and 1 : 2 complexes.

3.7 Aqueous spectral studies of VO(acac-NMe_2)$_2$

Dissolution of crystalline VO(acac-NMe_2)$_2$ (3.10 mM, pH 3.8) in distilled water showed two species by EPR spectra. The minor species (≈10%) has the parameters $A_0 = 99 \times 10^{-4}$ cm^{-1}, $g_0 = 1.972$ and is assigned to the 1 : 1 species (data not shown). The major species (≈90%) is assigned to VO^{2+} ($A_0 = 106 \times 10^{-4}$ cm^{-1}, $g_0 = 1.964$).[24] The parameters for the minor species are similar to those observed for VO(acac-NH_2)$_2$, confirming the hydrolysis of VO(acac-NMe_2)$_2$ in aqueous solution to the 1 : 1 species and VO^{2+}; no other species was observed at pH 3.8. Interestingly, the VO(acac-NMe_2)$_2$ complex is not only more soluble than the parent system in organic solvents, but also more soluble in aqueous solution. The addition of excess of ligand decreased the concentration of VO^{2+} and increased concentration of the 1 : 1 species. At 50 mM excess ligand the 1 : 1 species became the major species. An additional species (1 : 2 species) was observed in the presence of 864 mM excess ligand at pH 5.25 (Fig. 5). The existence of the 1 : 2 species was confirmed by potentiometry as described above and by recording the EPR spectrum in the presence of high levels of ligand at basic pH (see Fig. 5 for spectrum at pH 9.2).

Quantitative EPR studies were carried out to examine the speciation. In solutions of crystalline VO(acac-NMe_2)$_2$ only about 15–20% of the vanadium(IV) added to the solution was visible by EPR spectroscopy. The combination of quantitative EPR and ^{51}V NMR showed that, in solutions in the absence of large amounts of ligand, significant concentration of EPR-silent vanadium(IV) formed, presumably in the form of soluble vanadium(IV)–hydroxo complexes. Dissolution of crystalline VO(acac-NMe_2)$_2$ in solutions of free Hacac-NMe_2 generated solutions with increasing vanadium(IV) species as evidenced by the decreasing signal to noise in the spectra with excess of free ligand (data not shown). In solutions containing 204 and 436 mM excess ligand, a total of 90 and 97%, respectively, of the added vanadium(IV) was observed. Although, qualitatively, the solution properties of the VO(acac-NMe_2)$_2$ species are similar to those observed for VO(acac-NH_2)$_2$, the VO(acac-NMe_2)$_2$ complex is less stable than VO(acac-NH_2)$_2$ as observed by potentiometry.

Evidence for both the major 1 : 1 and minor 1 : 2 species also was sought by UV-visible spectroscopy. Solutions of crystalline VO(acac-NMe_2)$_2$ gave a spectrum similar to that obtained

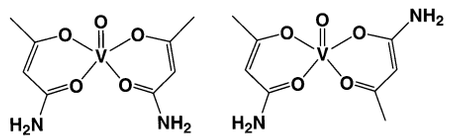

Fig. 7 The two possible structures for C_s symmetric and C_2 symmetric 1 : 2 VO(acac-NH_2)$_2$.

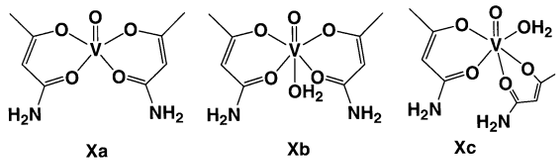

Fig. 8 Three out of four possible structures for the symmetric 1 : 2 VO(acac-NH_2)$_2$ complex; the C_s parent structure (**Xa**), the *trans* H_2O adduct (**Xb**) and the *cis* H_2O adduct (**Xc**).

for VO(acac-NH_2)$_2$ and distinct from the spectrum observed for $VOSO_4$ at the same pH.[24] However, when crystalline VO(acac-NMe_2)$_2$ was dissolved in solutions containing 436 mM Hacac-NMe_2, two absorbance maxima at 567 and 803 nm were observed (Fig. 6). By EPR spectroscopy, this solution was found to contain 3.61 mM 1 : 1 species and 0.20 mM 1 : 2 species. Solutions of crystalline VO(acac-NMe_2)$_2$ in the presence of large excesses of ligand at pH 9.2 were found to contain only the 1 : 2 species (Fig. 5). Surprisingly, the UV-visible spectra of these solutions were very similar to that observed for solutions containing the 1 : 1 species (Fig. 6). Since the solutions containing VO(acac-NMe_2)$_2$ accounted for all the vanadium(IV) added, the observed spectra represent the EPR observable species. However, at alkaline pH, a mixed hydroxo complex VO(acac-NMe_2)$_2$(OH) may form (presumably as a *trans* adduct, see below), which could contribute to the observed UV-visible spectrum. If OH coordinated in the apical position *trans* to the oxo group, EPR parameters should not be affected by this deprotonation.[24] Spectra (some of which are depicted in Fig. 6) recorded at identical pH values were unable satisfactorily to resolve this issue because such solutions did not contain sufficient EPR-active species to account for all the vanadium(IV) added. The absorbance spectra shown in Fig. 6 therefore are likely to also include spectral contributions from EPR silent vanadyl hydroxo species in addition to VO(acac-NMe_2)$_2$ species.

3.8 Structures for 1 : 1 and 1 : 2 complexes

The asymmetry of the amide ligands allowed formation of 1 : 2 complexes in which the ligands are coordinated to the vanadium with the amide groups *cis* (C_s symmetry) or *trans* (C_2 symmetry) (Fig. 7). Although previous reports refer to the C_2 type geometry for vanadium(IV) complexes,[33] the X-ray crystallographic structure for VO(acac-NMe_2)$_2$ provides precedence for the C_s symmetric structure. Thus, we assume that the solution geometries have ligands coordinated *cis*. Upon dissolution in water and organic solvents a solvent molecule can coordinate to the 1 : 2 complex. Studies by UV-vis spectroscopy suggest that VO(acac)$_2$ forms an adduct with water (containing six-coordinate vanadium) and EPR parameters suggest that H_2O is coordinated *trans* to the oxo group in the major species and *cis* to the oxo group in the minor species.[25] Four possible structures exist for the C_s symmetric ligand coordinated 1 : 2 VO(acac-NH_2)$_2$ and VO(acac-NMe_2)$_2$ complexes; the C_s parent structure (**Xa** and **Ya**), the *trans* H_2O adduct (**Xb** and **Yb**) and the two *cis* H_2O adducts (**Xc** and **Yc/Xd** and **Yd**). Correspondingly four structures can be shown for the C_2 symmetric complexes; Fig. 8 shows structures **Xa**, **Xb** and **Xc**.

The 100 nm red shift of the absorbance band for VO(acac)$_2$ (about 660–680 nm) is indicative of solvent coordination

Table 5 Summary of the structural assignment for the $VO(acac\text{-}NR_2)_2$ and $VO(acac)_2$ complexes in the solid state and in solution

Complex	Solid state	UV-Vis			EPR
		Water	Pyridine	DMF and DMSO	
$VO(acac\text{-}NH_2)_2$ R = H	**N/A**	**Xb/Xc**[a]	**Xb/Xc**[a]	**Xa**	**Xa/Xb**[a]
$VO(acac\text{-}NMe_2)_2$ R = Me	**Ya**	**Yb/Yc**[a]	**Yb/Yc**[a]	**Ya**	**Ya/Yb**[a]
$VO(acac)_2$[b]	**Za**[c,d]	**Zb**[e]**/Zc**[a,c,e]	**Zb**[c]**/Zc**[a,c,e]	**Zb**[c]**/Zc**[a,c,e]	**Za**[c]**/Zb**[a,c] and **Zc**[c,e]

[a] The notation **Xb/Xc** is used to indicate that the method cannot distinguish between the two indicated structures. The fourth possible structure **Xd** (or **Zd**) is less likely than **Xc** (or **Zc**) and is not discussed further. [b] Refs. 25, 31. [c] **Za**, **Zb** and **Zc** are defined for $VO(acac)_2$ analogous to the structures **Xa**, **Xb** and **Xc**. [d] Although the structure **Za** is not observed in the solvents indicated in this table, it forms in non-coordinating solvents such as benzene and nitromethane. In less coordinating solvents such as acetone, 1,4-dioxane and CH_3CN mixtures of **Za** and **Zb/Zc** form (see *b*). [e] **Zc** is only with certainty observed in aqueous solution.

to the vanadium atom *trans* to the oxo group.[31] EPR spectroscopy is sensitive when a ligand in the equatorial plane is substituted.[25] The combination of EPR and UV-visible spectroscopic parameters measured in this work thus provides excellent structural characterization of the solution species and the assignments are summarized in Table 5. Since the absorbance peak at about 680 nm of the two $VO(acac\text{-}NR_2)_2$ complexes did not shift in most organic solvents, the solution complex is **Xa** and **Ya**. In contrast, in water the absorbances are about 800 nm consistent with the solution structures in water being **Xb** and **Yb**, respectively. The EPR parameters for the $VO(acac\text{-}NH_2)_2$ complex vary in the solvents examined as the parameters for $VO(acac)_2$ vary. However, the A_0 values for **Xa** and **Xb** and **Ya** and **Yb**, respectively, are likely to be similar given the fact that axial ligands have little effect on the EPR parameters. Combined these facts are consistent with the interpretation that the 1 : 2 species for the $VO(acac\text{-}NR_2)_2$ complexes observed in aqueous solution is the *trans* H_2O adduct.

The recent speciation studies of the $VO(acac)_2$ system also revealed the existence of a *cis* H_2O adduct.[25,32] These structures are represented by **Xc** and **Yc** in (**Xc** shown in Fig. 8) for the $VO(acac\text{-}NR_2)_2$ systems. No evidence for the *cis* adducts was observed by EPR spectroscopy for the amide complexes, suggesting the concentration of such species is below the detection limit. The UV-visible absorbance band in the past has exclusively been attributed to the *trans* solvent adduct;[31] however, the lack of spectroscopic data prevents convincing distinction between the *cis* and *trans* adducts.

In addition to the 1 : 2 species the 1 : 1 species also forms in solutions. It is only observed in aqueous solution. The A_0 values for this species for the $VO(acac\text{-}NR_2)_2$ systems and the $VO(acac\text{-}R)_2$ systems are experimentally indistinguishable. However, the UV-visible spectra show some differences. Combined these facts suggest that the solution structure of the 1 : 1 species formed from $VO(acac\text{-}NH_2)_2$ differs from that formed from $VO(acac)_2$. Based on the absorption spectrum, the $VO(acac)_2$ species contains a five-coordinate vanadium atom whereas the $VO(acac\text{-}NMe_2)_2$ contains a six-coordinate vanadium atom.

3.9 Oxidation products as monitored by ^{51}V NMR spectroscopy

Aqueous solutions of crystalline $VO(acac\text{-}NH_2)_2$ and $VO(acac\text{-}NMe_2)_2$ (pH 3.8–3.9) upon standing within an hour generated solutions containing small amounts of decavanadate as determined by ^{51}V NMR spectroscopy. In contrast, solutions of crystalline $VO(acac\text{-}NH_2)_2$ and $VO(acac\text{-}NMe_2)_2$ in the presence of a 100-fold excess of ligand (pH 3.8–3.9) oxidized at a significantly slower rate, but in the course of one-week vanadium(v) species were observed. Faster rates of oxidation were observed at neutral pH in the absence of excess of ligand; immediately after dissolution >80% of the vanadium(IV) had converted into vanadium(v) and was observed as decavanadate.

4.0 Conclusion

Two new heteroatom-containing $VO(acac)_2$ derived complexes were prepared and characterized in organic and in aqueous solutions. The complexes are stable in organic solvents such as DMF, DMSO and pyridine, and depending on the coordinating abilities of the solvent will exist as a five- or six-coordinate species. Depending on the pH, the dissolved crystalline compound dissociates and hydrolyzes and the vanadium oxidizes. However, both 1 : 1 and 1 : 2 complexes are fairly stable under appropriately chosen pH and in the presence of an excess of ligand. Based on our studies, the 1 : 2 $VO(acac\text{-}NMe_2)_2$ complex is slightly less stable than the parent $VO(acac\text{-}NH_2)_2$ in aqueous media, but both are less stable than $VO(acac)_2$. However, the ratio of the 1 : 1 complex to the 1 : 2 complex is higher for the amide complexes than for the parent and alkylated $VO(acac)_2$ complexes. Should the 1 : 1 species be crucial for insulin-like properties of these $VO(acac)_2$ derived complexes it may be mechanistically useful further to elucidate the mode by which these compounds act.

Acknowledgements

The work was supported by the Institute of General Medical Sciences at The National Institutes of Health (to D. C. C.), the National Scientific Research Fund (to T. K.) and by the Hungarian Ministry of Education (to T. K.).

5.0 References

1 J. H. McNeill, V. G. Yuen, H. R. Hoveyda and C. Orvig, *J. Med. Chem.*, 1992, **35**, 1489.
2 P. Kinetek, *Phase 1 Study of KP-102*, in *CNW-PRN*, Newsedge Corporation, Vancouver, 1998.
3 V. G. Yuen, P. Caravan, L. Gelmini, N. Glover, J. H. McNeill, I. A. Setyawati, Y. Zhou and C. Orvig, *J. Inorg. Biochem.*, 1997, **68**, 109.
4 B. A. Reul, S. S. Amin, J. P. Buchet, L. N. Ongemba, D. C. Crans and S. M. Brichard, *Br. J. Pharm.*, 1999, **126**, 467.
5 H. Watanabe, M. Nakai, K. Komazawa and H. Sakurai, *J. Med. Chem.*, 1994, **37**, 876.
6 H. Sakurai, K. Fujii, H. Watanabe and H. Tamura, *Biochem. Biophys. Res. Commun.*, 1995, **214**, 1095.
7 K. Kawabe, M. Tadokoro, Y. Kojima, Y. Fujisawa and H. Sakurai, *Chem. Lett.*, 1998, 9.
8 H. Sakurai, K. Tsuchiya, M. Nukatsuka, J. Kawada, S. Ishikawa, H. Yoshida and M. Komatsu, *J. Clin. Biochem. Nutr.*, 1990, **8**, 193.
9 A. S. Tracey and D. C. Crans, *ACS Symp. Ser.*, 1998, **711**.
10 G. T. Morgan and H. W. Moss, *J. Chem. Soc.*, 1914, **103**, 78.
11 R. P. Dodge, D. H. Templeton and A. Zalkin, *J. Chem. Phys.*, 1961, **35**, 55.
12 K. Kaneda, K. Jitsukawa, T. Itoh and S. Teranishi, *J. Org. Chem.*, 1980, **45**, 3004.
13 T. Hirao, *Chem. Rev.*, 1997, **97**, 2707.
14 P. A. Wender, K. D. Rice and M. E. Schnute, *J. Am. Chem. Soc.*, 1997, **119**, 7897.
15 P. K. Hon, R. L. Belford and C. E. Pfluger, *J. Chem. Phys.*, 1965, **43**, 1323.

16 A. J. Tasiopoulos, A. T. Vlahos, A. D. Keramidas, T. A. Kabanos, Y. G. Deligiannakis, C. P. Raptopoulou and A. Terzis, *Angew. Chem., Int. Ed. Engl.*, 1996, **35**, 2531.
17 A. D. Keramidas, A. B. Papaioannou, A. Vlahos, T. A. Kabanos, G. Bonas, A. Makriyannis, C. P. Raptopoulou and A. Terzis, *Inorg. Chem.*, 1996, **35**, 357.
18 G. Gran, *Acta Chem. Scand.*, 1950, **4**, 559.
19 G. M. Sheldrick, SADABS (a Program for Siemens Area Detection Absorption Correction), Book *SADABS (a Program for Siemens Area Detection Absorption Correction)*, to be published; G. M. Sheldrick, SHELXTL, Siemens Analytical X-Ray Diffraction, Book *SHELXTL, Siemens Analytical X-Ray Diffraction*, Siemens, Madison, WI, 1996, vol. 5.
20 I. Nagypal and I. Fabian, *Inorg. Chim. Acta*, 1982, **61**, 109.
21 H. Irving, M. G. Miles and L. D. Pettit, *Anal. Chim. Acta*, 1967, **38**, 475.
22 Y. L. Zekany and I. Nagypal, in *Computational Methods for the Determination of Formation Constants*, ed. D. J. Leggett, Plenum Press, New York, 1985.
23 R. P. Henry, P. C. Mitchell and J. E. Prue, *J. Chem. Soc., Dalton Trans.*, 1973, 1156; A. Komura, M. Hayashi and H. Imanaga, *Bull. Chem. Soc. Jpn.*, 1977, **50**, 2927.
24 N. D. Chasteen, in *Biological Magnetic Resonance*, eds. L. Berliner and J. Reuben, Plenum Press, New York, 1981, pp. 53–119.
25 S. S. Amin, K. Cryer, B. Zhang, S. K. Dutta, S. S. Eaton, O. P. Anderson, S. M. Miller, B. A. Reul, S. M. Brichard and D. C. Crans, *Inorg. Chem.*, 2000, **39**, 406.
26 R. S. Drago, *Physical Methods for Chemists*, Saunders College Publishing, Orlando, 1992, p. 750.
27 R. A. Rowe and M. M. Jones, *Inorg. Synth.*, 1957, **5**, 113.
28 R. C. Paul, S. Bhatia and A. Kumar, *Inorg. Synth.*, 1971, **13**, 181.
29 J. Selbin, *Coord. Chem. Rev.*, 1966, **1**, 293.
30 L. J. Boucher, E. C. Tynan and T. F. Yen, in *Electron Spin Resonance of Metal Complexes*, ed. T. F. Yen, Plenum Press, New York, 1969, pp. 111–130.
31 W. Linert, E. Herlinger, P. Margl and R. Boca, *J. Coord. Chem.*, 1993, **28**, 1.
32 D. C. Crans, T. Kiss and T. Jakusch, 2000, to be submitted.
33 H. Sakurai, Z. E. Taira and N. Sakai, *Inorg. Chim. Acta*, 1988, **151**, 85.